

# Surface Engineering of Graphene-Based Nanomaterials for Biomedical Applications

Sixiang Shi,<sup>†</sup> Feng Chen,<sup>‡</sup> Emily B. Ehlerding,<sup>§</sup> and Weibo Cai<sup>\*,†,‡,§,||</sup>

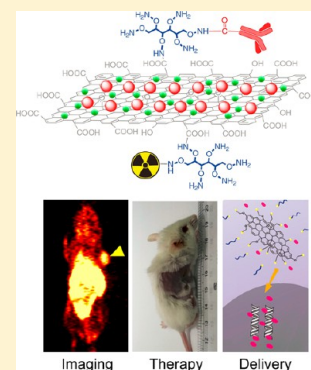
<sup>†</sup>Materials Science Program, University of Wisconsin—Madison, Madison, Wisconsin 53706, United States

<sup>‡</sup>Department of Radiology, University of Wisconsin—Madison, Madison, Wisconsin 53792, United States

<sup>§</sup>Department of Medical Physics, University of Wisconsin—Madison, Madison, Wisconsin 53705, United States

<sup>||</sup>University of Wisconsin Carbone Cancer Center, Madison, Wisconsin 53792, United States

**ABSTRACT:** Graphene-based nanomaterials have attracted tremendous interest over the past decade due to their unique electronic, optical, mechanical, and chemical properties. However, the biomedical applications of these intriguing nanomaterials are still limited due to their suboptimal solubility/biocompatibility, potential toxicity, and difficulties in achieving active tumor targeting, just to name a few. In this Topical Review, we will discuss in detail the important role of surface engineering (i.e., bioconjugation) in improving the in vitro/in vivo stability and enriching the functionality of graphene-based nanomaterials, which can enable single/multimodality imaging (e.g., optical imaging, positron emission tomography, magnetic resonance imaging) and therapy (e.g., photothermal therapy, photodynamic therapy, and drug/gene delivery) of cancer. Current challenges and future research directions are also discussed and we believe that graphene-based nanomaterials are attractive nanoplateforms for a broad array of future biomedical applications.



## ■ INTRODUCTION

Graphene, an emerging nanomaterial with single-layered carbon atoms in two dimensions, has attracted tremendous interest since 2004, due to its unique electronic, optical, mechanical, and chemical properties.<sup>1–7</sup> Among different subtypes of graphene-based nanomaterials, graphene oxide (GO) and reduced graphene oxide (RGO) have been widely studied in the realm of nanomedicine.<sup>8</sup> Owing to their extremely high specific surface area, GO and RGO have been reported to be able to interact with various molecules, such as doxorubicin (DOX) and polyethylenimine (PEI), and have been accepted as excellent platforms for drug delivery and gene transfection.<sup>9–16</sup>

Surface engineering of graphene-based nanomaterials has played a vital role in their biomedical applications.<sup>7,8,17</sup> For example, suitable PEGylation could not only improve the solubility and biocompatibility of GO, but also reduce its potential toxicity in vitro as well as in vivo.<sup>18–20</sup> After integration with other functional nanoparticles, such as magnetic iron oxide nanoparticles (IONPs),<sup>21–24</sup> gold nanoparticles,<sup>25–27</sup> and quantum dots (QDs),<sup>28–30</sup> functionalized GO and RGO have also shown great potential for simultaneous cancer imaging and therapy in small animals.<sup>30–34</sup> With the conjugation of well-selected targeting ligands, tumor targeted GO (or RGO) has already shown significantly enhanced tumor accumulation in different cancer models in vivo.<sup>35–37</sup> Scheme 1 summarizes representative processes of surface functionalization of GO and RGO. In this chapter, we will focus on surface engineering of GO and RGO for biomedical applications.

## ■ SYNTHESIS OF GRAPHENE-BASED NANOMATERIALS

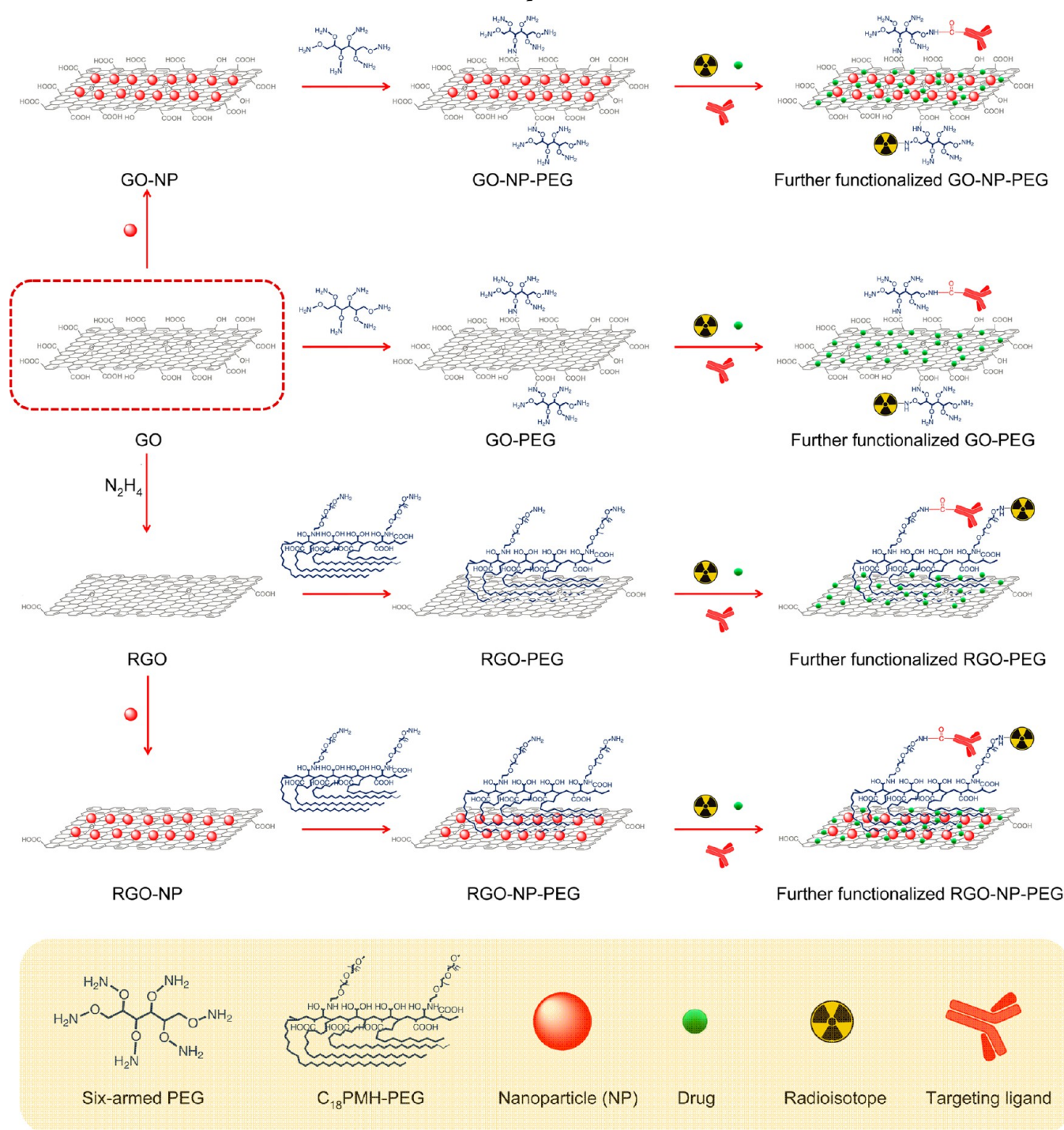
Generally, two methods have been developed for the synthesis of graphene. The first method is a top-down approach, which could cleave multilayer graphite into single layers via mechanical, physical, or chemical exfoliation.<sup>38–40</sup> The second method is a bottom-up approach, wherein graphene could be obtained by chemical vapor deposition of one-layer carbon onto well-selected substrates.<sup>41–43</sup>

So far, oxidative exfoliation via the Hummers method (developed by Hummers and Offeman in 1950s) is the most popular method for the generation of graphene derivatives, such as GO, with great output.<sup>44</sup> This technique involves the oxidative exfoliation of graphite using a mixture of potassium permanganate (KMnO<sub>4</sub>) and concentrated sulfuric acid (H<sub>2</sub>SO<sub>4</sub>). As-produced GO is highly oxidized with a large number of residual epoxides, hydroxides and carboxylic acid groups on its surface. To restore the structure and properties of graphene, GO could be further reduced to obtain RGO by reacting with well-selected reducing agents (e.g., N<sub>2</sub>H<sub>4</sub>).<sup>45</sup> In comparison with GO, RGO is known to have increased conductive and optical absorbance, making it a more attractive agent for future cancer photothermal therapy.<sup>31</sup> For more detailed information about the synthesis of graphene-based nanomaterials, readers are referred to these excellent review papers.<sup>40,41</sup>

**Received:** July 24, 2014

**Revised:** August 5, 2014

**Published:** August 13, 2014

Scheme 1. Schematic Illustration of Functionalization of Graphene-Based Nanomaterials<sup>a</sup>

<sup>a</sup>Reproduced with permission from ref 17.

## ■ SURFACE ENGINEERING OF GRAPHENE-BASED NANOMATERIALS

**To Improve Biocompatibility.** As we have mentioned, GO has abundant epoxides, hydroxides, and carboxylic acid groups on its surface, which makes it possible for covalent surface functionalization based on these reactive groups. Polyethylene glycol (PEG) is among the most widely used for improving the solubility and biocompatibility of graphene derivatives.<sup>18,46,47</sup> By using amine-terminated branched PEG, successful PEGylation of GO has been reported (Figure 1A).<sup>10</sup>

Intensive sonication was first introduced to break larger GO (size range: 50–500 nm) down to nanographene oxide (nGO) with a significantly reduced size range (i.e., 5–50 nm) (Figure 1B). Six-armed branched PEG was then covalently linked to the carboxylic acid groups on nGO using well-established EDC (1-ethyl-3-(3-(dimethylamino)propyl)carbodiimide)/NHS (*N*-hydroxysuccinimide) chemistry. The resulting PEGylated nGO (nGO-PEG) exhibited superior stability in biological solutions (Figure 1C). The same PEGylation strategy has been widely used for surface modification of other GO-based nanoparticles,



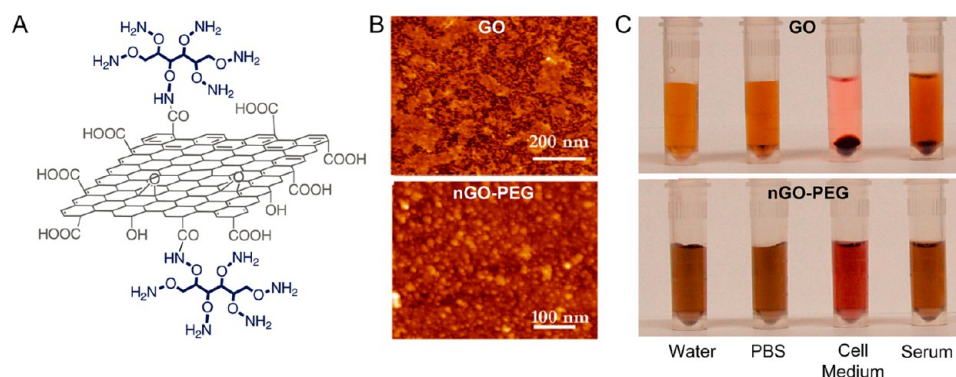


**Figure 1.** Covalent functionalization of GO by six-armed branched PEG. (A) Schematic illustration of PEGylated GO. (B) Atomic force microscope (AFM) image of GO (top) and nGO-PEG (bottom). (C) Photos of GO (top) and nGO-PEG (bottom) in different solutions recorded after centrifugation at 10000g for 5 min. GO crashed out slightly in PBS and completely in cell medium and serum while nGO-PEG was stable in all solutions. Reproduced with permission from ref 10 and 17.

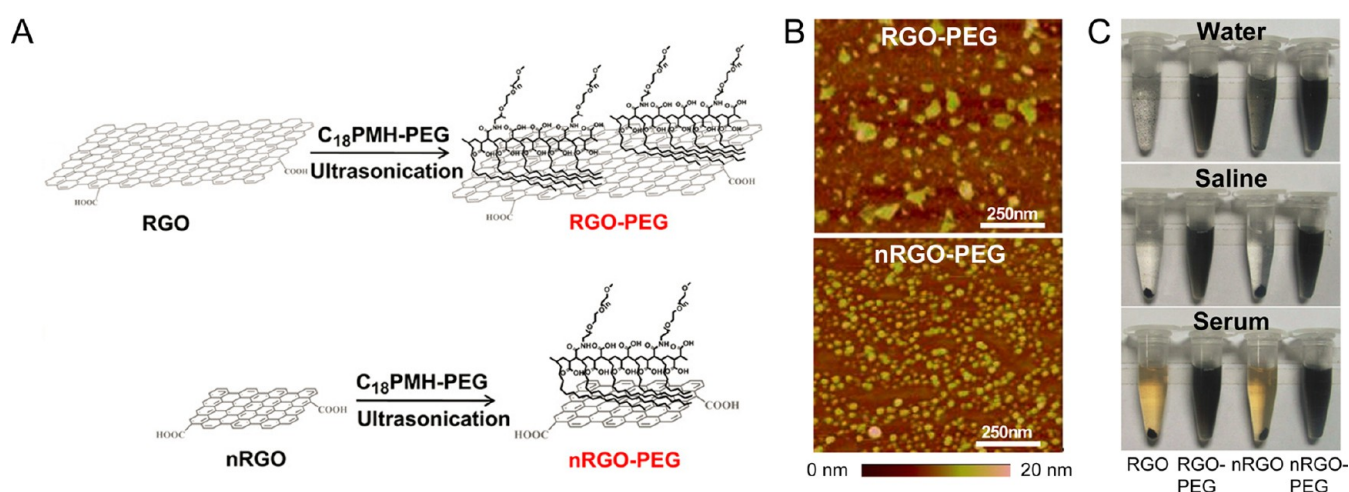


**Figure 2.** Noncovalent surface functionalization of RGO with  $C_{18}$ PMH-PEG. (A) Schematic illustration of PEGylated RGO and nRGO. (B) AFM images of RGO-PEG (top) and nRGO-PEG (bottom). (C) Photos of RGO, RGO-PEG, nRGO, and nRGO-PEG in water (top), saline (middle), and fetal bovine serum (bottom). RGO and nRGO aggregated slightly in water and completely in saline and serum, whereas RGO-PEG and nRGO-PEG are stable in all solutions. Reproduced with permission from ref 31.

and has shown reduced toxicity in vitro.<sup>19,48–52</sup> Besides enhanced biocompatibility and reduced toxicity, GO coated with amine-terminated PEG could also provide abundant amino groups for the further bioconjugations.

Many other hydrophilic polymers, including poly(L-lysine) (PLL),<sup>53</sup> poly(acrylic acid) (PAA),<sup>54</sup> dextran,<sup>55,56</sup> and chitosan,<sup>57–60</sup> have also been studied for surface functionalization of GO. In one study, GO was functionalized with PLL by stirring GO solution with PLL in the presence of potassium hydroxide (KOH), and subsequently treated with sodium borohydride ( $NaBH_4$ ).<sup>53</sup> As-synthesized PLL functionalized GO showed high solubility and biocompatibility, and contained plentiful amino groups. In another work, PAA-coated GO was synthesized via intensive sonication and microwave irradiation.<sup>54</sup> Functionalization of PAA could not only improve the biocompatibility of GO but also work as a bridge for linking the fluorescein *o*-methacrylate (FMA), resulting in fluorescent GO for optical imaging.

Besides covalent surface modification, noncovalent coating via hydrophobic interactions,  $\pi$ - $\pi$  stacking, and electrostatic interactions are other effective approaches to enabling improved solubility and biocompatibility of graphene derivatives.<sup>8</sup> The attachment of PEGylated phospholipids on RGO

was completed in one of the first studies of this kind.<sup>61</sup> In a follow-up study, PEG-grafted poly(maleic anhydride-*alt*-1-octadecene) (i.e.,  $C_{18}$ PMH-PEG) was used for nano RGO (nRGO) surface modification via strong hydrophobic interactions between the hydrophobic graphene surface and long hydrocarbon chains in the  $C_{18}$ PMH-PEG polymer (Figure 2A and B).<sup>31</sup> The solubility of RGO and nRGO in physiological solutions was found to be dramatically enhanced after coating (Figure 2C). In addition,  $C_{18}$ PMH-PEG coating was also found helpful for prolonging the blood circulation half-life of functionalized nRGO.<sup>62,63</sup> Other agents, including bovine serum albumin (BSA),<sup>52</sup> polyoxyethylene sorbitan laurate (Tween),<sup>64</sup> Pluronic F127 (PF127),<sup>65,66</sup> polyethylenimine (PEI),<sup>48</sup> and cholesteryl hyaluronic acid (CHA),<sup>12</sup> have also been used for noncovalent surface functionalization of graphene derivatives.

#### Cancer Imaging with Graphene-Based Nanomaterials.

Molecular imaging holds great potential in drug development, disease diagnosis, therapeutic responses monitoring, and the understanding of complex interactions between nanomedicine and living biological systems.<sup>67–69</sup> In the past several years, enormous efforts have been devoted to surface engineering of different graphene derivatives for studying their in vivo

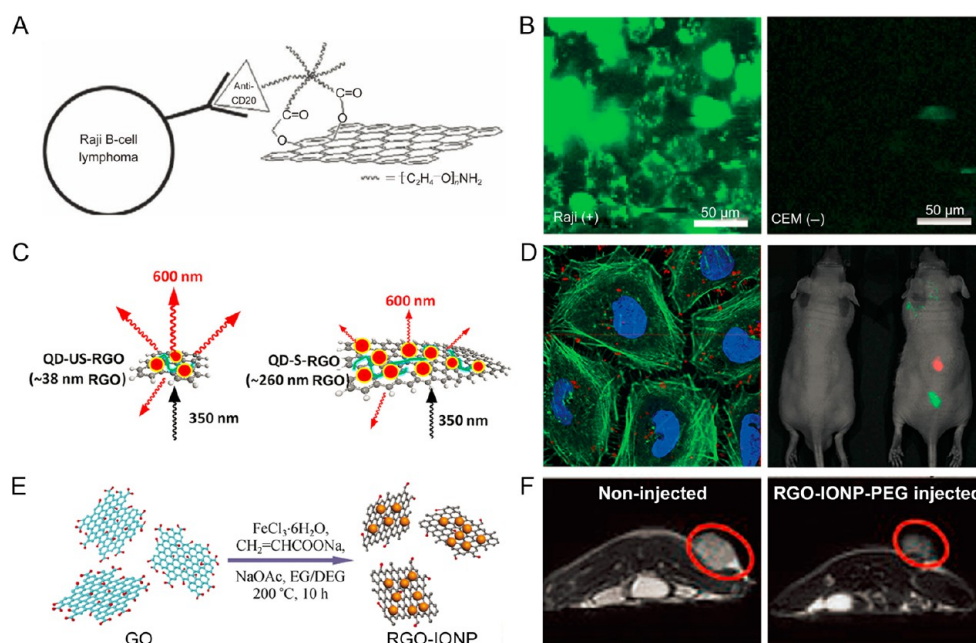


**Figure 3.** Functionalization of graphene for cancer imaging. (A) Schematic drawing illustrating nGO-PEG conjugated with anti-CD20 antibody Rituxan. (B) NIR fluorescence image of nGO-PEG-Rituxan conjugate in CD20 positive cells (left) and negative cells (right). (C) Schematic illustration of shielding effect of RGO for the two sizes, absorbing more incoming irradiation and stimulating less QD fluorescence by the larger RGO. (D) Optical imaging exhibiting locations of the QD-US-RGO within the cells (left) and mouse (right). (E) Schematic illustration of synthesis of RGO-IONP. (F)  $T_2$ -weighted MR imaging of noninjected mouse (left) and injected mouse (right) with RGO-IONP-PEG. Reproduced with permission from refs 30, 34, 47, and 88.

biodistribution patterns and tumor targeting efficacy using imaging modalities such as optical imaging,<sup>28,29,47,70–79</sup> positron emission tomography (PET),<sup>35–37,76,80</sup> magnetic resonance imaging (MRI),<sup>21–24,34,81–83</sup> and others.

**Optical Imaging.** Optical imaging is an inexpensive, widely available, and highly sensitive imaging technique.<sup>84–86</sup> By using the intrinsic photoluminescence of nGO in the near-infrared (NIR) range, nGO was functionalized with PEG and Rituxan anti-CD20 (a B-cell specific antibody) to form nGO-PEG-Rituxan and examined in the range of 1100–2200 nm (Figure 3A).<sup>47</sup> Optical imaging demonstrated the specific uptake of nGO-PEG-Rituxan in Raji B-cell surfaces (CD20 positive), but not in CEM T-cells (CD20 negative) (Figure 3B). Due to the relatively low autofluorescence, excellent image contrast could be obtained.

Besides intrinsic photoluminescence, various fluorescent labels such as organic dyes<sup>18,74</sup> and QDs<sup>28–30</sup> have been functionalized on graphene for optical imaging. For example, a commonly used NIR fluorescent dye (i.e., Cy7) was conjugated to nGO-PEG for in vivo optical imaging in mice bearing different kinds of tumors (i.e., 4T1 murine breast cancer tumors, KB human epidermoid carcinoma tumors, and U87MG human glioblastoma tumors).<sup>18</sup>

Conjugating QDs (or other optical imaging nanoparticles)<sup>79</sup> onto RGO could also result in fluorescent RGO provided that optical quenching is efficiently suppressed.<sup>28–30</sup> For example, tri-*n*-octylphosphine oxide (TOPO) protected QDs were attached onto RGO-PLL, resulting in RGO-PLL-QD with effectively reduced fluorescence quenching.<sup>30</sup> Interestingly, QD-loaded ultrasmall RGO sheets (i.e., QD-US-RGO) demonstrated a decreased fluorescence quenching when compared with QD-loaded larger RGO sheets (QD-S-RGO) (Figure 3C). The imaging property was tested in cells and mice (Figure 3D), demonstrating that both size and surface

modification play important roles in the optical imaging of QD integrated graphene.

**PET Imaging.** PET is a highly sensitive and quantitative imaging modality and could become a useful imaging tool for studying the in vivo fate of graphene-based nanomaterial after radiolabeling.<sup>84,85,87</sup> So far, radioisotopes such as copper-64 ( $^{64}\text{Cu}$ ,  $t_{1/2} = 12.7$  h) have been labeled to GO (or RGO) for in vivo biodistribution and targeting studies.<sup>35,37,76,80</sup> In one study, GO was modified with 2-(1-hexyloxyethyl)-2-devinyl pyrophosphoribide- $\alpha$  (HPPH), which could bind to  $^{64}\text{Cu}$  for PET imaging via passive targeting.<sup>76</sup> Higher tumor uptake was achieved with HPPH modified GO in comparison with HPPH alone, indicating the successful in vivo passive targeting. In another study, we reported the synthesis of  $^{64}\text{Cu}$ -labeled GO and RGO by using NOTA (i.e., 1,4,7-triazacyclononane-1,4,7-triacetic acid) as the chelator.<sup>35,37</sup> For example, rapid and persistent tumor uptake was achieved with  $^{64}\text{Cu}$ -labeled GO and peaked at 3 h post injection ( $>5\%$ ID/g) with excellent image contrast, suggesting the potential of graphene-based nanomaterials for PET imaging in preclinical studies and future applications.<sup>35</sup> Since in vivo active targeting has been successfully achieved, this study will be discussed in detail in a later section.

**Magnetic Resonance Imaging.** Iron oxide nanoparticles (IONPs) are well-studied  $T_2$  contrast agents, and have been decorated to GO or RGO using different strategies.<sup>23,24,34</sup> In one study, IONPs were decorated onto GO via chemical deposition using soluble GO as carriers, where  $\text{Fe}^{3+}/\text{Fe}^{2+}$  ions with a proper ratio were captured by carboxylate anions on the graphene sheet by coordination, forming IONPs on GO after treatment with NaOH solution at 65 °C.<sup>21</sup> In follow-up study, a simple in situ method for decorating RGO with monodisperse IONPs was reported by reacting iron(III) acetylacetonate ( $\text{Fe}(\text{acac})_3$ ) in liquid polyol triethylene glycol (TREG) at high



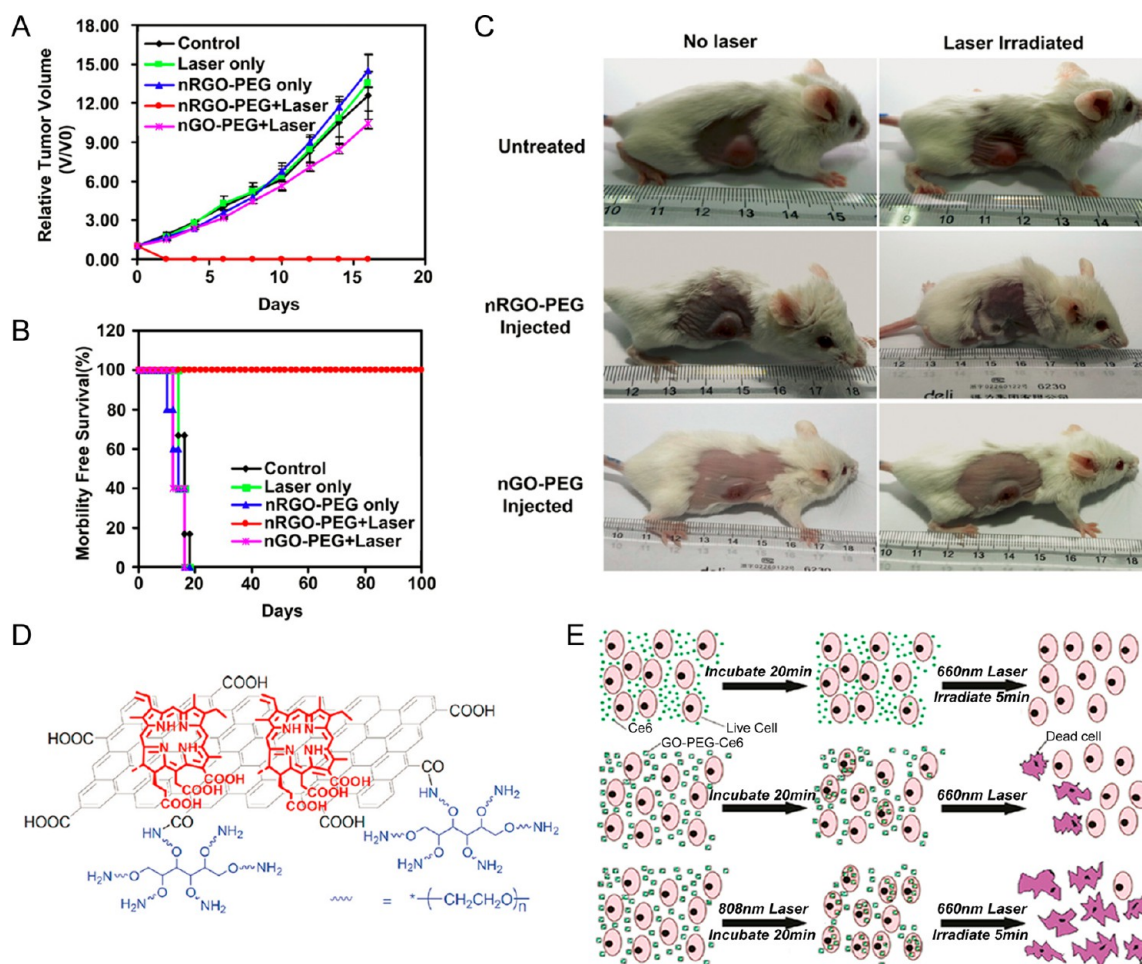


**Figure 4.** Photothermal therapy and photodynamic therapy with functionalized graphene. (A) Tumor growth curves of different groups of mice after treatment. The tumor volumes were normalized to their initial sizes. (B) Survival curves of mice bearing 4T1 tumors after various treatments indicated. nRGO-PEG injected mice after PTT treatment survived over 100 days without a single death. (C) Representative photos of tumor-bearing mice after various treatments indicated. The laser irradiated tumors on the nRGO-PEG injected mice were completely destroyed. Laser wavelength = 808 nm. Power density = 0.15 W/cm<sup>2</sup>. Irradiation time = 5 min. (D) Schematic illustration showing Ce6 loading on GO-PEG. Red: Ce6; black: GO; blue: six-arm PEG. (E) Schemes of the experimental design in photothermally enhanced photodynamic therapy. Free Ce6 (top) and GO-PEG-Ce6 (middle) for 20 min in the dark and then irradiated by the 660 nm laser (50 mW/cm<sup>2</sup>, 5 min, 15 J/cm<sup>2</sup>) for PDT in control experiments; GO-PEG-Ce6 incubated cells were exposed to the 808 nm laser (0.3 W/cm<sup>2</sup>, 20 min, 360 J/cm<sup>2</sup>) first (bottom) to induce PTT before PDT treatment. Reproduced with permission from refs 31 and 105.

temperature.<sup>22</sup> The distribution of IONPs on the RGO sheet was found to be uniform with no obvious magnetic particle aggregation. Furthermore, in another interesting study, GO-IONP-PEG was synthesized by the reduction reaction between FeCl<sub>3</sub> and diethylene glycol (DEG) in the presence of NaOH at high temperature and MRI with enhanced T<sub>2</sub>-weighted MR images was then achieved in mice, suggesting that integrated graphene could be an excellent platform for in vivo MRI (Figure 3E and F).<sup>34,88</sup> Besides IONPs, gadolinium (Gd)-based complexes have also been conjugated to GO for enhanced T<sub>1</sub>-weighted MR imaging.<sup>82</sup>

**Other Imaging Modalities.** Functionalized GO has attracted extensive interest in photoacoustic (PA) imaging for non-invasive imaging of tissue structures and functions, due to its strong NIR light absorbance.<sup>89</sup> It was proven that the PA signal (under a laser pulse of 808 nm) remained strong at a depth of 11 mm and gradually weakened as the detection depth increased in ex vivo studies.<sup>90</sup> In vivo PA imaging has also been accomplished in mice model.<sup>34,91</sup> Raman imaging is another application of graphene-based nanomaterials, due to

the inherent Raman signals.<sup>92</sup> It was discovered that the inherent Raman signals were significantly enhanced after integration of metal nanoparticles with graphene-based nanomaterials.<sup>93,94</sup> The integrated nanoparticles (e.g., GO-Au or GO-Ag NPs) have been tested in living cells as sensitive optical probes.<sup>95–97</sup> Besides, single-photon emission computed tomography (SPECT) has also been applied for tumor imaging with graphene-based nanomaterials.<sup>98</sup> However, considering the higher sensitivity of PET over SPECT,<sup>99</sup> most of current radiolabeled studies have been focused on PET imaging.

**Photothermal Therapy and Photodynamic Therapy.** PEGylated GO (i.e., GO-PEG) is one of the first reported graphene derivatives designed for in vivo photothermal therapy (PTT), and showed highly efficient tumor ablation under NIR light irradiation (808 nm, 2 W/cm<sup>2</sup>).<sup>18</sup> No obvious side effects of GO-PEG were noticed during the treatment. To further improve the PTT efficiency, in a follow-up study, RGO with a more restored graphene structure was utilized by the same group.<sup>31</sup> PEGylated ultras-small nRGO (i.e., nRGO-PEG) with an average size of 27 nm was prepared. Systematic in vivo PTT

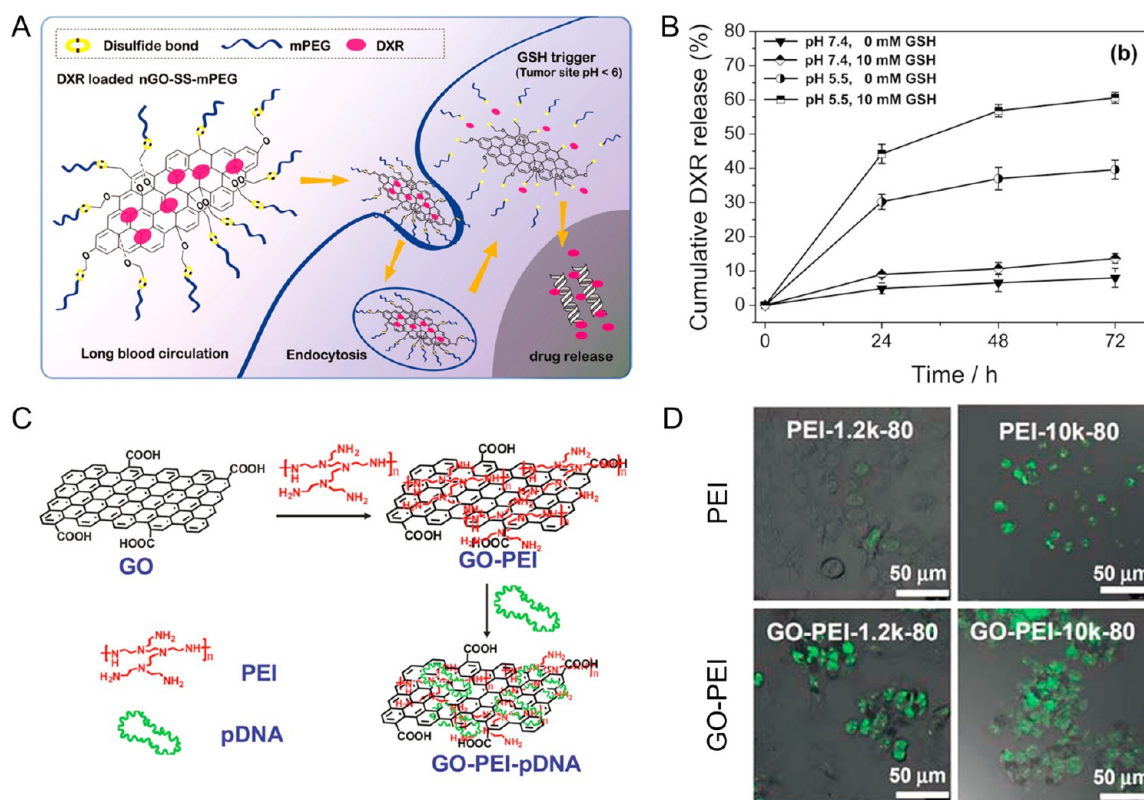


**Figure 5.** Functionalization of GO for drug and gene delivery. (A) Schematic diagram showing antitumor activity of redox-sensitive Doxorubicin (DXR)-loaded nGO-SS-mPEG. (B) GSH-mediated drug release from DXR-loaded nGO-SS-mPEG at pH 7.4 and 5.5. Higher release rate was achieved in the presence of GSH at pH 5.5. (C) Schematic illustration showing the synthesis of GO-PEI conjugate and the preparation of GO-PEI-pDNA complex. (D) Confocal images of PEI and GO-PEI transfected HeLa cells with two different molecular weights of PEI (N/P ratio = 80). Reproduced with permission from refs 9 and 107.

study demonstrated highly efficient tumor ablation under significantly reduced NIR laser power density ( $0.15 \text{ W/cm}^2$ ) and improved survival (Figure 4A,B,C), indicating RGO could be one of the best candidates for PTT with a low-power laser irradiation. Besides pure GO, nanoparticle-decorated GO has also been reported for synergistic enhanced PTT. For example, gold nanoparticles (or nanorods) were attached onto GO resulting in enhanced PTT effects.<sup>25,26</sup> Other nanoparticles such as silver (Ag),<sup>100</sup> copper(I) oxide ( $\text{Cu}_2\text{O}$ ),<sup>101</sup> and copper monosulfide ( $\text{CuS}$ )<sup>102</sup> have also been integrated with GO for similarly enhanced PTT.

Photodynamic therapy (PDT) is another recognized alternative for the treatment of various cancers by triggering the generation of reactive oxygen species (ROS) through the interaction of light with selected photosensitizers (PSs).<sup>103</sup> PSs such as zinc phthalocyanine (ZnPc), Chlorin e6 (Ce6), and others have been loaded on the surface of GO-PEG for PDT studies in vitro and in vivo.<sup>32,104</sup> For example, research showed that Chlorin e6 (Ce6) could be attached to the surface of GO via hydrophobic interactions and  $\pi$ - $\pi$  stacking.<sup>32</sup> As-synthesized GO-Ce6 nanosheets showed increased accumulation of Ce6 in tumor cells and could lead to a remarkable photodynamic efficacy upon light irradiation (633 nm). A PTT/PDT combined therapy could also be achieved by using GO-PEG-Ce6 (Figure 4D).<sup>105</sup> Significantly enhanced therapeutic outcome was observed when compared with either PDT or PTT alone (Figure 4E), highlighting the attractive potential of combined phototherapy using graphene-based nanomaterials.

**Drug and Gene Delivery.** Graphene-based nanomaterials can also be used for drug and gene delivery.<sup>46,106</sup> The strong  $\pi$ - $\pi$  interaction allows for the loading of various aromatic drug molecules such as doxorubicin (DOX)<sup>13,20,47,107</sup> and camptothecin (CPT),<sup>13,57,108</sup> while hydrophobic interaction provides a chance to bind to numerous poorly water-soluble drugs, such as paclitaxel, without compromising their potency or efficiency.<sup>109</sup> By appropriate surface coating with PEI or chitosan, as functionalized graphene could also be used for effective gene delivery.<sup>8,46,110</sup>

DOX was loaded on to nGO-PEG by simply mixing the two together at pH 8 environment via  $\pi$ - $\pi$  stacking to form nGO-PEG-DOX.<sup>47</sup> A similar loading mechanism was used for the synthesis of nGO-PEG-SN38 (SN38 is an analogue of CPT).<sup>10</sup> The resulting nGO-PEG-SN38 complex exhibited excellent water solubility while maintaining a high chemotherapeutic potency similar to that of the free SN38 molecules. In addition to single drug loading, nGO can be used for loading multiple drugs for chemotherapy. For example, both DOX and CPT were loaded on functionalized nGO and showed higher cytotoxicity to cancer cells compared to nGO loaded with DOX or CPT alone.<sup>13</sup> More sophisticated surface engineering techniques have also been reported for achieving on-demand drug release functionality. For example, disulfide linkages were introduced to PEGylated GO to form nGO-SS-mPEG (mPEG = methoxy polyethylene glycol) (Figure 5A).<sup>107</sup> PEG was able to selectively detach from nGO upon intracellular glutathione (GSH) stimulation and effectively accelerate the drug release at lower pH (Figure 5B). In a recent study, GO was modified with



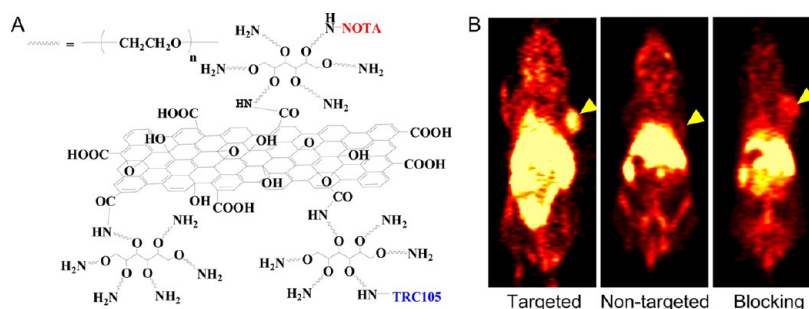


**Figure 6.** Conjugation of targeting ligands for tumor active targeting. (A) Schematic representation of the nanographene conjugates with NOTA as the chelator for in vivo imaging and TRC105 as the targeting ligand. (B) Coronal PET images of 4T1 tumor-bearing mice at 3 h postinjection of  $^{64}\text{Cu}$ -NOTA-GO-TRC105 (targeted),  $^{64}\text{Cu}$ -NOTA-GO (nontargeted), or  $^{64}\text{Cu}$ -NOTA-GO-TRC105 after a preinjected blocking dose of TRC105 (blocking). Enhanced tumor uptake was achieved with  $^{64}\text{Cu}$ -NOTA-GO-TRC105 compared with nontargeting and blocking groups. Reproduced with permission from ref 35.

2,3-dimethylmaleic anhydride (DA), which is negatively charged under physiological pH at 7.4 and could be rapidly converted into positively charged moiety in a slightly acidic environment (pH 6.8).<sup>111</sup> Significantly enhanced pH-responsive drug release and improved therapeutic efficacy were achieved in cells. Overall, these studies demonstrated the potential of using graphene-based nanomaterials for loading and delivery of aromatic and/or hydrophobic drugs.

The development of nanoparticle-based gene delivery is still limited by the immunogenicity and potential cytotoxicity of gene carriers.<sup>112,113</sup> Successful loading and intracellular transfection of plasmid DNA (pDNA) in HeLa cells has been reported recently by using PEI functionalized GO (Figure 5C).<sup>9</sup> Results showed that the chain length of PEI could have a significant influence on the transfection rate and cellular toxicity. GO-PEI-1.2k exhibited higher transfection efficiency than PEI-1.2k, while GO-PEI-10k exhibited lower cellular toxicity than PEI-10k (Figure 5D). This work demonstrated that GO could potentially become an effective platform for further applications in nonviral gene therapy. In addition, under irradiation with NIR light beam, enhanced cellular uptake was achieved due to mild photothermal heating, which increased the cell membrane permeability.<sup>110</sup> Besides pDNA, small interfering RNA (siRNA) was also delivered with nGO-PEG-PEI.<sup>15,110</sup>

**In Vivo Tumor Targeting with Graphene-Based Nanomaterials.** Although graphene-based nanomaterials have shown attractive potential for future cancer imaging and therapy, it is still a major challenge to improve their in vivo tumor targeting efficiency.<sup>114–117</sup> In comparison with passive and tumor cell-based targeting strategies, tumor angiogenesis targeting (or vasculature targeting) has recently been accepted as a generally applicable in vivo targeting strategy for most nanoparticles regardless of tumor types.<sup>118</sup>

CD105, also known as endoglin, is an ideal marker for tumor angiogenesis since it is almost exclusively expressed on proliferating endothelial cells.<sup>119</sup> Recently, by using TRC105 (a human/murine chimeric IgG1 monoclonal antibody that binds to both human and murine CD105),<sup>120,121</sup> we reported the first example of in vivo active targeted PET imaging of well-designed GO and RGO nanoconjugates (Figure 6A).<sup>35–37</sup> Significantly higher uptake in 4T1 murine breast tumors (which express high level of CD105 on the tumor vasculature) was observed for TRC105-conjugated GO, which was about 2-fold that for the nontargeted GO (Figure 6B). Enhanced tumor uptake with high specificity and little extravasation was achieved

in this study, encouraging future investigation of these GO conjugates for cancer-targeted drug delivery and/or PTT to enhance therapeutic efficacy.

## CONCLUSION AND FUTURE PERSPECTIVES

Over the past decade, great efforts have been made to employ functionalized graphene-based nanomaterials in biomedical applications. Optical imaging has been widely studied via either intrinsic fluorescence of graphene or integrating fluorescent dyes and nanoparticles. Although optical imaging is limited by limited tissue penetration and quenching from graphene, the undesired quenching could possibly be utilized for engineering of activatable fluorescent probes for on-demand imaging with enhanced contrast. Compared with optical imaging, PET and MRI could become better candidates for future in vivo imaging due to their excellent tissue penetration property. For therapy, PTT, PDT, and drug (or gene) delivery have proven to be efficient and effective methods with reduced side effects to normal tissues, where the surface engineering plays an important role in the therapeutic efficacy. With sophisticated surface engineering, graphene-based nanomaterials could be designed as multifunctional probes for multimodality image-guided therapy, which would be one of the most promising research directions in the next 5 years.

Despite recent progress in surface engineering of graphene-based nanomaterials for biomedical applications, challenges still exist. Among them, potential long-term toxicity and unsatisfactory tumor targeting efficacy are two of the major concerns. As discussed, surface functionalization plays a critical role in improving the solubility and biocompatibility of graphene-based nanomaterials. By modification with various biocompatible molecules, significantly improved stability and reduced toxicity have been achieved. Although PEGylation has been accepted as the best surface modification method, due to the relatively large size and nonbiodegradable property of graphene-based nanomaterials, the high liver uptake and potential long-term toxicity are still major concerns for future clinical translation. Second, although enhanced GO (or RGO) accumulation has been demonstrated with the assistance of well-selected antibodies, so far the tumor targeting efficacy is still relatively low (5–8%ID/g). The development of new tumor targeting strategies, better tumor targeting ligands and bioconjugation techniques will be highly useful for the engineering of the next generation of graphene-based nanomaterials.

In conclusion, we summarized the functionalization of graphene-based nanomaterials for various biomedical applications. With appropriate surface engineering techniques, graphene and its derivatives could be used for cancer multimodality imaging, photothermal therapy, photodynamic therapy, drug and gene delivery, cancer active targeting, and other applications.

## AUTHOR INFORMATION

### Corresponding Author

\*E-mail: WCai@uwhealth.org. Phone: +1 (608) 262-1749. Fax: +1 (608) 265-0614.

### Notes

The authors declare no competing financial interest.

## ACKNOWLEDGMENTS

This work is supported, in part, by the University of Wisconsin - Madison, the National Institutes of Health (NIBIB/NCI 1R01CA169365), the Department of Defense (W81XWH-11-1-0644), and the American Cancer Society (125246-RSG-13-099-01-CCE).

## REFERENCES

- (1) Novoselov, K. S.; Geim, A. K.; Morozov, S. V.; Jiang, D.; Zhang, Y.; Dubonos, S. V.; Grigorieva, I. V.; and Firsov, A. A. (2004) Electric field effect in atomically thin carbon films. *Science* 306, 666–9.
- (2) Geim, A. K., and Novoselov, K. S. (2007) The rise of graphene. *Nat. Mater.* 6, 183–91.
- (3) Huang, X., Yin, Z., Wu, S., Qi, X., He, Q., Zhang, Q., Yan, Q., Boey, F., and Zhang, H. (2011) Graphene-based materials: synthesis, characterization, properties, and applications. *Small* 7, 1876–902.
- (4) Li, X., Wang, X., Zhang, L., Lee, S., and Dai, H. (2008) Chemically derived, ultrasmooth graphene nanoribbon semiconductors. *Science* 319, 1229–32.
- (5) Pumera, M. (2010) Graphene-based nanomaterials and their electrochemistry. *Chem. Soc. Rev.* 39, 4146–57.
- (6) Service, R. F. (2009) Materials science. Carbon sheets an atom thick give rise to graphene dreams. *Science* 324, 875–7.
- (7) Zhang, Y., Nayak, T. R., Hong, H., and Cai, W. (2012) Graphene: a versatile nanopatform for biomedical applications. *Nanoscale* 4, 3833–42.
- (8) Yang, K., Feng, L., Shi, X., and Liu, Z. (2013) Nano-graphene in biomedicine: theranostic applications. *Chem. Soc. Rev.* 42, 530–47.
- (9) Feng, L., Zhang, S., and Liu, Z. (2011) Graphene based gene transfection. *Nanoscale* 3, 1252–7.
- (10) Liu, Z., Robinson, J. T., Sun, X., and Dai, H. (2008) PEGylated nanographene oxide for delivery of water-insoluble cancer drugs. *J. Am. Chem. Soc.* 130, 10876–7.
- (11) Kim, H., Lee, D., Kim, J., Kim, T. I., and Kim, W. J. (2013) Photothermally triggered cytosolic drug delivery via endosome disruption using a functionalized reduced graphene oxide. *ACS Nano* 7, 6735–46.
- (12) Miao, W., Shim, G., Kang, C. M., Lee, S., Choe, Y. S., Choi, H. G., and Oh, Y. K. (2013) Cholesteryl hyaluronic acid-coated, reduced graphene oxide nanosheets for anti-cancer drug delivery. *Biomaterials* 34, 9638–47.
- (13) Zhang, L., Xia, J., Zhao, Q., Liu, L., and Zhang, Z. (2010) Functional graphene oxide as a nanocarrier for controlled loading and targeted delivery of mixed anticancer drugs. *Small* 6, 537–44.
- (14) Tang, L. A., Wang, J., and Loh, K. P. (2010) Graphene-based SELDI probe with ultrahigh extraction and sensitivity for DNA oligomer. *J. Am. Chem. Soc.* 132, 10976–7.
- (15) Zhang, L., Lu, Z., Zhao, Q., Huang, J., Shen, H., and Zhang, Z. (2011) Enhanced chemotherapy efficacy by sequential delivery of siRNA and anticancer drugs using PEI-grafted graphene oxide. *Small* 7, 460–4.
- (16) He, S., Song, B., Li, D., Zhu, C., Qi, W., Wen, Y., Wang, L., Song, S., Fang, H., and Fan, C. (2010) A graphene nanoprobe for rapid, sensitive, and multicolor fluorescent DNA analysis. *Adv. Funct. Mater.* 20, 453–459.
- (17) Yang, K., Feng, L., Hong, H., Cai, W., and Liu, Z. (2013) Preparation and functionalization of graphene nanocomposites for biomedical applications. *Nat. Protoc.* 8, 2392–403.
- (18) Yang, K., Zhang, S., Zhang, G., Sun, X., Lee, S. T., and Liu, Z. (2010) Graphene in mice: ultrahigh in vivo tumor uptake and efficient photothermal therapy. *Nano Lett.* 10, 3318–23.
- (19) Yang, K., Wan, J., Zhang, S., Zhang, Y., Lee, S. T., and Liu, Z. (2011) In vivo pharmacokinetics, long-term biodistribution, and toxicology of PEGylated graphene in mice. *ACS Nano* 5, 516–22.
- (20) Zhang, W., Guo, Z. Y., Huang, D. Q., Liu, Z. M., Guo, X., and Zhong, H. Q. (2011) Synergistic effect of chemo-photothermal therapy using PEGylated graphene oxide. *Biomaterials* 32, 8555–8561.
- (21) Yang, X. Y., Zhang, X. Y., Ma, Y. F., Huang, Y., Wang, Y. S., and Chen, Y. S. (2009) Superparamagnetic graphene oxide-Fe<sub>3</sub>O<sub>4</sub> nanoparticles hybrid for controlled targeted drug carriers. *J. Mater. Chem.* 19, 2710–2714.
- (22) Cong, H. P., He, J. J., Lu, Y., and Yu, S. H. (2010) Water-soluble magnetic-functionalized reduced graphene oxide sheets: in situ synthesis and magnetic resonance imaging applications. *Small* 6, 169–73.
- (23) He, H., and Gao, C. (2010) Supraparamagnetic, conductive, and processable multifunctional graphene nanosheets coated with high-density Fe<sub>3</sub>O<sub>4</sub> nanoparticles. *ACS Appl. Mater. Interfaces* 2, 3201–10.
- (24) He, F. A., Fan, J. T., Ma, D., Zhang, L. M., Leung, C., and Chan, H. L. (2010) The attachment of Fe<sub>3</sub>O<sub>4</sub> nanoparticles to graphene oxide by covalent bonding. *Carbon* 48, 3139–3144.
- (25) Zedan, A. F., Moussa, S., Terner, J., Atkinson, G., and El-Shall, M. S. (2013) Ultrasmall gold nanoparticles anchored to graphene and enhanced photothermal effects by laser irradiation of gold nanostructures in graphene oxide solutions. *ACS Nano* 7, 627–36.
- (26) Dembereldorj, U., Choi, S. Y., Ganbold, E. O., Song, N. W., Kim, D., Choo, J., Lee, S. Y., Kim, S., and Joo, S. W. (2014) Gold nanorod-assembled PEGylated graphene-oxide nanocomposites for photothermal cancer therapy. *Photochem. Photobiol.* 90, 659–66.
- (27) Jin, Y., Wang, J., Ke, H., Wang, S., and Dai, Z. (2013) Graphene oxide modified PLA microcapsules containing gold nanoparticles for ultrasonic/CT bimodal imaging guided photothermal tumor therapy. *Biomaterials* 34, 4794–802.
- (28) Chen, M. L., Liu, J. W., Hu, B., and Wang, J. H. (2011) Conjugation of quantum dots with graphene for fluorescence imaging of live cells. *Analyst* 136, 4277–83.
- (29) Chen, M. L., He, Y. J., Chen, X. W., and Wang, J. H. (2013) Quantum-dot-conjugated graphene as a probe for simultaneous cancer-targeted fluorescent imaging, tracking, and monitoring drug delivery. *Bioconjugate Chem.* 24, 387–397.
- (30) Hu, S. H., Chen, Y. W., Hung, W. T., Chen, I. W., and Chen, S. Y. (2012) Quantum-dot-tagged reduced graphene oxide nanocomposites for bright fluorescence bioimaging and photothermal therapy monitored in situ. *Adv. Mater.* 24, 1748–54.
- (31) Yang, K., Wan, J., Zhang, S., Tian, B., Zhang, Y., and Liu, Z. (2012) The influence of surface chemistry and size of nanoscale graphene oxide on photothermal therapy of cancer using ultra-low laser power. *Biomaterials* 33, 2206–14.
- (32) Huang, P., Xu, C., Lin, J., Wang, C., Wang, X., Zhang, C., Zhou, X., Guo, S., and Cui, D. (2011) Folic acid-conjugated graphene oxide loaded with photosensitizers for targeting photodynamic therapy. *Theranostics* 1, 240–50.
- (33) Zhou, L., Wang, W., Tang, J., Zhou, J. H., Jiang, H. J., and Shen, J. (2011) Graphene oxide noncovalent photosensitizer and its anticancer activity in vitro. *Chemistry* 17, 12084–91.
- (34) Yang, K., Hu, L., Ma, X., Ye, S., Cheng, L., Shi, X., Li, C., Li, Y., and Liu, Z. (2012) Multimodal imaging guided photothermal therapy using functionalized graphene nanosheets anchored with magnetic nanoparticles. *Adv. Mater.* 24, 1868–72.



- (35) Hong, H., Yang, K., Zhang, Y., Engle, J. W., Feng, L., Yang, Y., Nayak, T. R., Goel, S., Bean, J., Theuer, C. P., Barnhart, T. E., Liu, Z., and Cai, W. (2012) In vivo targeting and imaging of tumor vasculature with radiolabeled, antibody-conjugated nanographene. *ACS Nano* 6, 2361–70.
- (36) Hong, H., Zhang, Y., Engle, J. W., Nayak, T. R., Theuer, C. P., Nickles, R. J., Barnhart, T. E., and Cai, W. (2012) In vivo targeting and positron emission tomography imaging of tumor vasculature with (66)Ga-labeled nano-graphene. *Biomaterials* 33, 4147–56.
- (37) Shi, S., Yang, K., Hong, H., Valdovinos, H. F., Nayak, T. R., Zhang, Y., Theuer, C. P., Barnhart, T. E., Liu, Z., and Cai, W. (2013) Tumor vasculature targeting and imaging in living mice with reduced graphene oxide. *Biomaterials* 34, 3002–9.
- (38) Eda, G., and Chhowalla, M. (2010) Chemically derived graphene oxide: towards large-area thin-film electronics and optoelectronics. *Adv. Mater.* 22, 2392–415.
- (39) Cui, X., Zhang, C., Hao, R., and Hou, Y. (2011) Liquid-phase exfoliation, functionalization and applications of graphene. *Nanoscale* 3, 2118–26.
- (40) Dreyer, D. R., Park, S., Bielawski, C. W., and Ruoff, R. S. (2010) The chemistry of graphene oxide. *Chem. Soc. Rev.* 39, 228–40.
- (41) Park, S., and Ruoff, R. S. (2009) Chemical methods for the production of graphenes. *Nat. Nanotechnol.* 4, 217–24.
- (42) Lim, C. H., Nesladek, M., and Loh, K. P. (2014) Observing high-pressure chemistry in graphene bubbles. *Angew. Chem., Int. Ed. Engl.* 53, 215–9.
- (43) Lewis, A. M., Derby, B., and Kinloch, I. A. (2013) Influence of gas phase equilibria on the chemical vapor deposition of graphene. *ACS Nano* 7, 3104–17.
- (44) Hummers, W. S., and Offeman, R. E. (1958) Preparation of graphitic oxide. *J. Am. Chem. Soc.* 80, 1339–1339.
- (45) Pei, S. F., and Cheng, H. M. (2012) The reduction of graphene oxide. *Carbon* 50, 3210–3228.
- (46) Goenka, S., Sant, V., and Sant, S. (2014) Graphene-based nanomaterials for drug delivery and tissue engineering. *J. Controlled Release* 173, 75–88.
- (47) Sun, X., Liu, Z., Welsher, K., Robinson, J. T., Goodwin, A., Zaric, S., and Dai, H. (2008) Nano-graphene oxide for cellular imaging and drug delivery. *Nano Res.* 1, 203–212.
- (48) Wojtoniszak, M., Chen, X., Kalenczuk, R. J., Wajda, A., Lapczuk, J., Kurzewski, M., Drozdziak, M., Chu, P. K., and Borowiak-Palen, E. (2012) Synthesis, dispersion, and cytocompatibility of graphene oxide and reduced graphene oxide. *Colloids Surf., B* 89, 79–85.
- (49) Yang, K., Gong, H., Shi, X., Wan, J., Zhang, Y., and Liu, Z. (2013) In vivo biodistribution and toxicology of functionalized nano-graphene oxide in mice after oral and intraperitoneal administration. *Biomaterials* 34, 2787–95.
- (50) Tan, X., Feng, L., Zhang, J., Yang, K., Zhang, S., Liu, Z., and Peng, R. (2013) Functionalization of graphene oxide generates a unique interface for selective serum protein interactions. *ACS Appl. Mater. Interfaces* 5, 1370–7.
- (51) Wu, Q., Zhao, Y., Fang, J., and Wang, D. (2014) Immune response is required for the control of in vivo translocation and chronic toxicity of graphene oxide. *Nanoscale* 6, 5894–906.
- (52) Li, Y., Feng, L., Shi, X., Wang, X., Yang, Y., Yang, K., Liu, T., Yang, G., and Liu, Z. (2014) Surface coating-dependent cytotoxicity and degradation of graphene derivatives: towards the design of non-toxic, degradable nano-graphene. *Small* 10, 1544–54.
- (53) Shan, C., Yang, H., Han, D., Zhang, Q., Ivaska, A., and Niu, L. (2009) Water-soluble graphene covalently functionalized by biocompatible poly-L-lysine. *Langmuir* 25, 12030–3.
- (54) Gollavelli, G., and Ling, Y. C. (2012) Multi-functional graphene as an in vitro and in vivo imaging probe. *Biomaterials* 33, 2532–45.
- (55) Zhang, S. A., Yang, K., Feng, L. Z., and Liu, Z. (2011) In vitro and in vivo behaviors of dextran functionalized graphene. *Carbon* 49, 4040–4049.
- (56) Jin, R., Ji, X., Yang, Y., Wang, H., and Cao, A. (2013) Self-assembled graphene-dextran nanohybrid for killing drug-resistant cancer cells. *ACS Appl. Mater. Interfaces* 5, 7181–9.
- (57) Bao, H. Q., Pan, Y. Z., Ping, Y., Sahoo, N. G., Wu, T. F., Li, L., Li, J., and Gan, L. H. (2011) Chitosan-functionalized graphene oxide as a nanocarrier for drug and gene delivery. *Small* 7, 1569–1578.
- (58) Wang, C., Mallela, J., Garapati, U. S., Ravi, S., Chinnasamy, V., Girard, Y., Howell, M., and Mohapatra, S. (2013) A chitosan-modified graphene nanogel for noninvasive controlled drug release. *Nano-medicine* 9, 903–11.
- (59) Wang, Z. H., Zhou, C. F., Xia, J. F., Via, B., Xia, Y. Z., Zhang, F. F., Li, Y. H., and Xia, L. H. (2013) Fabrication and characterization of a triple functionalization of graphene oxide with Fe<sub>3</sub>O<sub>4</sub>, folic acid and doxorubicin as dual-targeted drug nanocarrier. *Colloids Surf., B* 106, 60–65.
- (60) Depan, D., Shah, J., and Misra, R. D. K. (2011) Controlled release of drug from folate-decorated and graphene mediated drug delivery system: Synthesis, loading efficiency, and drug release response. *Mater. Sci. Eng., C* 31, 1305–1312.
- (61) Robinson, J. T., Tabakman, S. M., Liang, Y., Wang, H., Casalongue, H. S., Vinh, D., and Dai, H. (2011) Ultrasmall reduced graphene oxide with high near-infrared absorbance for photothermal therapy. *J. Am. Chem. Soc.* 133, 6825–31.
- (62) Robinson, J. T., Welsher, K., Tabakman, S. M., Sherlock, S. P., Wang, H., Luong, R., and Dai, H. (2010) High performance in vivo near-IR (>1 μm) imaging and photothermal cancer therapy with carbon nanotubes. *Nano Res.* 3, 779–793.
- (63) Prencipe, G., Tabakman, S. M., Welsher, K., Liu, Z., Goodwin, A. P., Zhang, L., Henry, J., and Dai, H. (2009) PEG branched polymer for functionalization of nanomaterials with ultralong blood circulation. *J. Am. Chem. Soc.* 131, 4783–7.
- (64) Park, S., Mohanty, N., Suk, J. W., Nagaraja, A., An, J., Piner, R. D., Cai, W., Dreyer, D. R., Berry, V., and Ruoff, R. S. (2010) Biocompatible, robust free-standing paper composed of a TWEEN/graphene composite. *Adv. Mater.* 22, 1736–40.
- (65) Hu, H., Yu, J., Li, Y., Zhao, J., and Dong, H. (2012) Engineering of a novel pluronic F127/graphene nanohybrid for pH responsive drug delivery. *J. Biomed. Mater. Res., Part A* 100, 141–8.
- (66) Cheng, Q. Y., and Han, B. H. (2013) Supramolecular hydrogel based on graphene oxides for controlled release system. *J. Nanosci. Nanotechnol.* 13, 755–60.
- (67) James, M. L., and Gambhir, S. S. (2012) A molecular imaging primer: modalities, imaging agents, and applications. *Physiol. Rev.* 92, 897–965.
- (68) Liu, H., Wu, Y., Wang, F., and Liu, Z. (2014) Molecular imaging of integrin αvβ3 expression in living subjects. *Am. J. Nucl. Med. Mol. Imaging* 4, 333–45.
- (69) Nolting, D. D., Nickels, M. L., Guo, N., and Pham, W. (2012) Molecular imaging probe development: a chemistry perspective. *Am. J. Nucl. Med. Mol. Imaging* 2, 273–306.
- (70) Wate, P. S., Banerjee, S. S., Jalota-Badwar, A., Mascarenhas, R. R., Zope, K. R., Khandare, J., and Misra, R. D. K. (2012) Cellular imaging using biocompatible dendrimer-functionalized graphene oxide-based fluorescent probe anchored with magnetic nanoparticles. *Nanotechnology* 23, 415101.
- (71) Dong, H., Li, Y., Yu, J., Song, Y., Cai, X., Liu, J., Zhang, J., Ewing, R. C., and Shi, D. (2013) A versatile multicomponent assembly via beta-cyclodextrin host-guest chemistry on graphene for biomedical applications. *Small* 9, 446–56.
- (72) Nurunnabi, M., Khatun, Z., Reeck, G. R., Lee, D. Y., and Lee, Y. K. (2013) Near infra-red photoluminescent graphene nanoparticles greatly expand their use in noninvasive biomedical imaging. *Chem. Commun. (Camb.)* 49, 5079–81.
- (73) Nurunnabi, M., Khatun, Z., Nafujjaman, M., Lee, D. G., and Lee, Y. K. (2013) Surface coating of graphene quantum dots using mussel-inspired polydopamine for biomedical optical imaging. *ACS Appl. Mater. Interfaces* 5, 8246–8253.
- (74) Feng, D., Song, Y. C., Shi, W., Li, X. H., and Ma, H. M. (2013) Distinguishing folate-receptor-positive cells from folate-receptor-negative cells using a fluorescence off-on nanoprobe. *Anal. Chem.* 85, 6530–6535.

- (75) Gao, Y., Zou, X., Zhao, J. X., Li, Y., and Su, X. (2013) Graphene oxide-based magnetic fluorescent hybrids for drug delivery and cellular imaging. *Colloids Surf., B* 112, 128–33.
- (76) Rong, P., Yang, K., Srivastan, A., Kiesewetter, D. O., Yue, X., Wang, F., Nie, L., Bhirde, A., Wang, Z., Liu, Z., Niu, G., Wang, W., and Chen, X. (2014) Photosensitizer loaded nano-graphene for multi-modality imaging guided tumor photodynamic therapy. *Theranostics* 4, 229–39.
- (77) Kosuge, H., Sherlock, S. P., Kitagawa, T., Terashima, M., Barral, J. K., Nishimura, D. G., Dai, H., and McConnell, M. V. (2011) FeCo/graphite nanocrystals for multi-modality imaging of experimental vascular inflammation. *PLoS One* 6, e14523.
- (78) Wu, X., Tian, F., Wang, W. X., Chen, J., Wu, M., and Zhao, J. X. (2013) Fabrication of highly fluorescent graphene quantum dots using L-glutamic acid for in vitro/in vivo imaging and sensing. *J. Mater. Chem. C* 1, 4676–4684.
- (79) Wang, Y., Wang, H., Liu, D., Song, S., Wang, X., and Zhang, H. (2013) Graphene oxide covalently grafted upconversion nanoparticles for combined NIR mediated imaging and photothermal/photodynamic cancer therapy. *Biomaterials* 34, 7715–24.
- (80) Sun, Z., Huang, P., Tong, G., Lin, J., Jin, A., Rong, P., Zhu, L., Nie, L., Niu, G., Cao, F., and Chen, X. (2013) VEGF-loaded graphene oxide as theranostics for multi-modality imaging-monitored targeting therapeutic angiogenesis of ischemic muscle. *Nanoscale* 5, 6857–66.
- (81) Romero-Aburto, R., Narayanan, T. N., Nagaoka, Y., Hasumura, T., Mitcham, T. M., Fukuda, T., Cox, P. J., Bouchard, R. R., Maekawa, T., Kumar, D. S., Torti, S. V., Mani, S. A., and Ajayan, P. M. (2013) Fluorinated graphene oxide; a new multimodal material for biological applications. *Adv. Mater.* 25, 5632–7.
- (82) Zhang, M., Cao, Y., Chong, Y., Ma, Y., Zhang, H., Deng, Z., Hu, C., and Zhang, Z. (2013) Graphene oxide based theranostic platform for T1-weighted magnetic resonance imaging and drug delivery. *ACS Appl. Mater. Interfaces* 5, 13325–32.
- (83) Gizzatov, A., Keshishian, V., Guven, A., Dimiev, A. M., Qu, F., Muthupillai, R., Decuzzi, P., Bryant, R. G., Tour, J. M., and Wilson, L. J. (2014) Enhanced MRI relaxivity of aquated Gd<sup>3+</sup> ions by carboxyphenylated water-dispersed graphene nanoribbons. *Nanoscale* 6, 3059–63.
- (84) Cai, W., and Chen, X. (2007) Nanoplateforms for targeted molecular imaging in living subjects. *Small* 3, 1840–54.
- (85) Massoud, T. F., and Gambhir, S. S. (2003) Molecular imaging in living subjects: seeing fundamental biological processes in a new light. *Genes Dev.* 17, 545–80.
- (86) Huang, X., Lee, S., and Chen, X. (2011) Design of "smart" probes for optical imaging of apoptosis. *Am. J. Nucl. Med. Mol. Imaging* 1, 3–17.
- (87) Lopci, E., Grassi, I., Chiti, A., Nanni, C., Cicoria, G., Toschi, L., Fonti, C., Lodi, F., Mattioli, S., and Fanti, S. (2014) PET radiopharmaceuticals for imaging of tumor hypoxia: a review of the evidence. *Am. J. Nucl. Med. Mol. Imaging* 4, 365–84.
- (88) Sun, H., Cao, L., and Lu, L. (2011) Magnetite/reduced graphene oxide nanocomposites: One step solvothermal synthesis and use as a novel platform for removal of dye pollutants. *Nano Res.* 4, 550–562.
- (89) Patel, M. A., Yang, H., Chiu, P. L., Mastrogiiovanni, D. D., Flach, C. R., Savaram, K., Gomez, L., Hemnarine, A., Mendelsohn, R., Garfunkel, E., Jiang, H., and He, H. (2013) Direct production of graphene nanosheets for near infrared photoacoustic imaging. *ACS Nano* 7, 8147–57.
- (90) Li, X.-D., Liang, X.-L., Yue, X.-L., Wang, J.-R., Li, C.-H., Deng, Z.-J., Jing, L.-J., Lin, L., Qu, E.-Z., Wang, S.-M., Wu, C.-L., Wu, H.-X., and Dai, Z.-F. (2014) Imaging guided photothermal therapy using iron oxide loaded poly(lactic acid) microcapsules coated with graphene oxide. *J. Mater. Chem. B* 2, 217–223.
- (91) Sheng, Z., Song, L., Zheng, J., Hu, D., He, M., Zheng, M., Gao, G., Gong, P., Zhang, P., Ma, Y., and Cai, L. (2013) Protein-assisted fabrication of nano-reduced graphene oxide for combined in vivo photoacoustic imaging and photothermal therapy. *Biomaterials* 34, 5236–43.
- (92) Fu, X., Bei, F., Wang, X., O'Brien, S., and Lombardi, J. R. (2010) Excitation profile of surface-enhanced Raman scattering in graphene-metal nanoparticle based derivatives. *Nanoscale* 2, 1461–6.
- (93) Xu, C., and Wang, X. (2009) Fabrication of flexible metal-nanoparticle films using graphene oxide sheets as substrates. *Small* 5, 2212–7.
- (94) Kim, Y. K., Na, H. K., Lee, Y. W., Jang, H., Han, S. W., and Min, D. H. (2010) The direct growth of gold rods on graphene thin films. *Chem. Commun. (Camb.)* 46, 3185–7.
- (95) Liu, Q., Wei, L., Wang, J., Peng, F., Luo, D., Cui, R., Niu, Y., Qin, X., Liu, Y., Sun, H., Yang, J., and Li, Y. (2012) Cell imaging by graphene oxide based on surface enhanced Raman scattering. *Nanoscale* 4, 7084–9.
- (96) Ma, X., Qu, Q., Zhao, Y., Luo, Z., Zhao, Y., Ng, K. W., and Zhao, Y. (2013) Graphene oxide wrapped gold nanoparticles for intracellular Raman imaging and drug delivery. *J. Mater. Chem. B* 1, 6495–6500.
- (97) Liu, Z., Guo, Z., Zhong, H., Qin, X., Wan, M., and Yang, B. (2013) Graphene oxide based surface-enhanced Raman scattering probes for cancer cell imaging. *Phys. Chem. Chem. Phys.* 15, 2961–6.
- (98) Cornelissen, B., Able, S., Kersemans, V., Waghorn, P. A., Myhra, S., Jurkshat, K., Crossley, A., and Vallis, K. A. (2013) Nanographene oxide-based radioimmunoconstructs for in vivo targeting and SPECT imaging of HER2-positive tumors. *Biomaterials* 34, 1146–54.
- (99) Rahmim, A., and Zaidi, H. (2008) PET versus SPECT: strengths, limitations and challenges. *Nucl. Med. Commun.* 29, 193–207.
- (100) Shi, J., Wang, L., Zhang, J., Ma, R., Gao, J., Liu, Y., Zhang, C., and Zhang, Z. (2014) A tumor-targeting near-infrared laser-triggered drug delivery system based on GO@Ag nanoparticles for chemo-photothermal therapy and X-ray imaging. *Biomaterials* 35, 5847–61.
- (101) Hou, C. Y., Quan, H. C., Duan, Y. R., Zhang, Q. H., Wang, H. Z., and Li, Y. G. (2013) Facile synthesis of water-dispersible Cu<sub>2</sub>O nanocrystal-reduced graphene oxide hybrid as a promising cancer therapeutic agent. *Nanoscale* 5, 1227–1232.
- (102) Bai, J., Liu, Y., and Jiang, X. (2014) Multifunctional PEG-GO/CuS nanocomposites for near-infrared chemo-photothermal therapy. *Biomaterials* 35, 5805–13.
- (103) Dolmans, D. E., Fukumura, D., and Jain, R. K. (2003) Photodynamic therapy for cancer. *Nat. Rev. Cancer* 3, 380–7.
- (104) Dong, H. Q., Zhao, Z. L., Wen, H. Y., Li, Y. Y., Guo, F. F., Shen, A. J., Frank, P., Lin, C., and Shi, D. L. (2010) Poly(ethylene glycol) conjugated nano-graphene oxide for photodynamic therapy. *Sci. China: Chem.* 53, 2265–2271.
- (105) Tian, B., Wang, C., Zhang, S., Feng, L., and Liu, Z. (2011) Photothermally enhanced photodynamic therapy delivered by nano-graphene oxide. *ACS Nano* 5, 7000–9.
- (106) Feng, L., and Liu, Z. (2011) Graphene in biomedicine: opportunities and challenges. *Nanomedicine (London)* 6, 317–24.
- (107) Wen, H., Dong, C., Dong, H., Shen, A., Xia, W., Cai, X., Song, Y., Li, X., Li, Y., and Shi, D. (2012) Engineered redox-responsive PEG detachment mechanism in PEGylated nano-graphene oxide for intracellular drug delivery. *Small* 8, 760–9.
- (108) Sahoo, N. G., Bao, H. Q., Pan, Y. Z., Pal, M., Kakran, M., Cheng, H. K. F., Li, L., and Tan, L. P. (2011) Functionalized carbon nanomaterials as nanocarriers for loading and delivery of a poorly water-soluble anticancer drug: a comparative study. *Chem. Commun. (Camb.)* 47, 5235–5237.
- (109) Arya, N., Arora, A., Vasu, K. S., Sood, A. K., and Katti, D. S. (2013) Combination of single walled carbon nanotubes/graphene oxide with paclitaxel: a reactive oxygen species mediated synergism for treatment of lung cancer. *Nanoscale* 5, 2818–29.
- (110) Feng, L., Yang, X., Shi, X., Tan, X., Peng, R., Wang, J., and Liu, Z. (2013) Polyethylene glycol and polyethylenimine dual-functionalized nano-graphene oxide for photothermally enhanced gene delivery. *Small* 9, 1989–97.
- (111) Feng, L., Li, K., Shi, X., Gao, M., Liu, J., and Liu, Z. (2014) Smart pH-responsive nanocarrier based on nano-graphene oxide for combined chemo- and photothermal therapy overcoming drug



resistance. *Advanced Healthcare Materials* [Online early access] DOI: 10.1002/adhm.201300549.

(112) Whitehead, K. A., Langer, R., and Anderson, D. G. (2009) Knocking down barriers: advances in siRNA delivery. *Nat. Rev. Drug. Discovery* 8, 129–38.

(113) Li, S. D., and Huang, L. (2006) Gene therapy progress and prospects: non-viral gene therapy by systemic delivery. *Gene Ther.* 13, 1313–9.

(114) Cai, W., Chen, K., Li, Z. B., Gambhir, S. S., and Chen, X. (2007) Dual-function probe for PET and near-infrared fluorescence imaging of tumor vasculature. *J. Nucl. Med.* 48, 1862–70.

(115) Cai, W., and Chen, X. (2008) Multimodality molecular imaging of tumor angiogenesis. *J. Nucl. Med.* 49 (Suppl 2), 113S–28S.

(116) Cai, W., Shin, D. W., Chen, K., Gheysens, O., Cao, Q., Wang, S. X., Gambhir, S. S., and Chen, X. (2006) Peptide-labeled near-infrared quantum dots for imaging tumor vasculature in living subjects. *Nano Lett.* 6, 669–76.

(117) Cai, W. B., and Chen, X. Y. (2008) Preparation of peptide-conjugated quantum dots for tumor vasculature-targeted imaging. *Nat. Protoc.* 3, 89–96.

(118) Chen, F., and Cai, W. (2014) Tumor vasculature targeting: a generally applicable approach for functionalized nanomaterials. *Small* 10, 1887–93.

(119) Seon, B. K., Haba, A., Matsuno, F., Takahashi, N., Tsujie, M., She, X., Harada, N., Uneda, S., Tsujie, T., Toi, H., Tsai, H., and Haruta, Y. (2011) Endoglin-targeted cancer therapy. *Curr. Drug Delivery* 8, 135–43.

(120) Rosen, L. S., Hurwitz, H. I., Wong, M. K., Goldman, J., Mendelson, D. S., Figg, W. D., Spencer, S., Adams, B. J., Alvarez, D., Seon, B. K., Theuer, C. P., Leigh, B. R., and Gordon, M. S. (2012) A phase I first-in-human study of TRC105 (Anti-Endoglin Antibody) in patients with advanced cancer. *Clin. Cancer Res.* 18, 4820–9.

(121) Orbay, H., Zhang, Y., Valdovinos, H. F., Song, G., Hernandez, R., Theuer, C. P., Hacker, T. A., Nickles, R. J., and Cai, W. (2013) Positron emission tomography imaging of CD105 expression in a rat myocardial infarction model with (64)Cu-NOTA-TRC105. *Am. J. Nucl. Med. Mol. Imaging* 4, 1–9.